Effects of end-user participation under a TSO-DSO coordination scheme for Norway

Dung-Bai Yen [*], Pedro Crespo del Granado, Maria Lavrutich

Department of Industrial Economics and Technology Management, Norwegian University of Science and Technology, Trondheim, Norway

ARTICLE INFO

ABSTRACT

This paper analyses the Norwegian Power System through a sequence of models that represents dynamics of the wholesale power market, distribution power network, end-users, and a coordination scheme between Transmission System Operators (TSOs) and Distribution System Operators (DSOs). The models assess the impact of end-user flexibility and TSO-DSO coordination on the power system's operation, with an emphasis on two research questions: the extent to which flexibility from end-users affects the power system's operation under the TSO-DSO coordination scheme, and the potential of the TSO-DSO coordination scheme in incentivizing end-users' flexibility. The paper presents three scenarios, involving varying degrees of coordination and end-user participation that are modeled and applied to the entire Norwegian power system. The results indicate that active end-user participation in the power market with a TSO-DSO coordination scheme could enhance the flexibility of the power system and support redispatch, while attaining a 14.5% redispatch cost reduction and 0.33% total system cost reduction. These findings offer insights for power system stakeholders concerning the potential advantages and challenges associated with fostering end-user flexibility and further developing TSO-DSO coordination schemes.

1. Introduction

As distributed power supply and demand, such as variable renewable energy (VRE) sources and electric vehicles, continue to expand, the active management within the distribution power network will become increasingly relevant for efficient power grid operation. In countries where transmission system operators (TSOs) and distributed system operators (DSOs) are separate entities, the necessity for coordination between them arises to ensure the safe and reliable operation of the power network at all levels.

To this end, TSO-DSO coordination have been proposed as a new approach to support congestion management or to raise flexibility services [1,2]. The introduction of these coordination schemes can give incentives to new niches at the distribution power network, such as active end-users who might be willing to participate in power markets with TSO-DSO coordination schemes. These actors can influence the operation and economic efficiency of the power system in return, and therefore affect the coordination scheme in the first place [3]. While the potential role of active end-users has been acknowledged, a comprehensive understanding of their impacts and resulting dynamics on system cost and operation is essential for optimizing power system operations, ensuring efficient resource allocation, and promoting sustainable energy consumption [4].

As a starting point for studying the aforementioned dynamics, it is worthwhile to investigate how the impacts will be if a TSO-DSO coordination scheme is introduced and active end-users are allowed, both from the system's perspective and from the end-users' perspective. To this end, we explore the following questions:

- To what extent will flexibility from end-users affect the operation of the power system under the TSO-DSO coordination scheme?
- How well will the TSO-DSO coordination scheme incentivize end-users flexibility?

To address these questions, we developed four models for the Norwegian power system, which corresponds to: (i) the end-users with high spatial resolution (Section 3.2), (ii) the distribution power network (Section 3.4), (iii) the Energy only Market (EOM) (Section 3.5.1), and (iv) the operations of the transmission grid (Section 3.5.2). The central underlying methodology of these models is based on mathematical programming commonly used in energy systems research. In these models, we implement three scenarios that cover various degrees of TSO-DSO coordination and end-user participation. The study places particular emphasis on the Norwegian power system, which is experiencing significant electrification across various sectors. This transition

---

* Corresponding author.
  E-mail address: dung.b.yen@ntnu.no (D.-B. Yen).

is characterized by a substantial increase in electricity demand, the installation of VRE sources, and high Electric Vehicle (EV) integration. The relatively comprehensive database of the power network sets Norway in a more favorable position compared with other countries for high spatial resolution power system modeling necessary to incorporate end-users into the study.

We find that the participation of active end-users has impacts on the costs in the power system. Specifically, during winter weeks, when active end-users support grid redispatch operations, their participation leads to a significant reduction in redispatch costs. By offering their flexibility, these end-users help balance the system, alleviating the need for costly interventions from other sources. However, it is important to note that their active participation in the EOM, when possible, introduces new dynamics. As active end-users change their demand profiles, it results in increased costs in the EOM. During summer weeks, end-users providing negative redispatch leads to an opposite direction of dynamics, one where the redispatch costs increase but costs in the EOM decrease, albeit to a lesser extent. Meanwhile, active end-users that provide flexibility to the power system can also reduce their average electricity prices in many parts of Norway. This is because participation of active end-users can smooth out spatial and temporal variations between supply and demand in the power system.

The findings offer a fresh outlook on the cost reduction and potential enhancement of system resilience resulting from the active involvement of end-users, thereby advocating for the implementation of new TSO-DSO coordination schemes that incorporate end-user participation. However, it is crucial for system operators and policymakers to consider the distributional impacts on relevant stakeholders that may arise as a consequence of these dynamics within the EOM and redispatch processes if active end-users are part of the system.

The rest of the paper is organized as follows: in Section 2 we review literature regarding TSO-DSO coordination and end-users' participation in power markets. In Section 3 we introduce the framework and methodology adopted for the model and the simulation. In Section 4 we present the results and insights. Section 5 concludes the paper and discusses potential future work.

2. Related literature

Distributed resources have the potential to offer significant flexibility services for the power system, including control reserve and congestion management, when granted the opportunity to participate in wholesale markets at the TSO level or local flexibility markets [5,6]. Traditionally the focus of distributed resources for these flexibility services has been on VRE sources, utility scale battery energy storage systems, and large energy consumers; end-users nevertheless can also provide flexibility for the power system via various models and strategies of demand side management [7,8].

TSO-DSO coordination schemes have emerged as a new mechanism to incorporate distributed resources into the existing power market [9]. Effective TSO-DSO coordination enables utilization of distributed resources, facilitates grid integration of renewable energy sources, and enhances the overall resilience and flexibility of the electricity grid [10]. However, the manner in which various TSO-DSO /coordination schemes are implemented can influence the extent of their market participation.

As examples, the SmartNet project has proposed five schemes for TSO-DSO coordination [11], with some leading to a higher level of involvement of DSOs in a local flexibility market while others assuming the distributed flexibility resources would directly participate in the transmission level flexibility market. In the study, the use of flexibility resources was shown to enable more options for DSOs to solve network issues, but liquidity might be a concern for local markets. [12] showed possible coordination and operation models of DSO flexibility markets, among which a Global and Local Ancillary Service Market platform was proposed in the paper the assign flexibility resources to the system

operator with highest priority. [13] formulated the bi-level optimization problem between the DSO and balance service providers in a local flexible market and calculated the reduction of balancing costs on a test system. It was shown that the hierarchy model enabled both TSO and DSO to utilize local resources, but the priority of DSO to use local resources might lead to sub-optimal solutions. [14] investigated a bi-level optimization problem between the TSO and the DSOs, and [15] proposed both an explicit local flexible market and an implicit network tariff for end-users to provide flexibility on the distribution grid. [16] proposed a new agent (the "interface optimizer") at the interface between DSOs and TSOs, so that it could optimize the coordination of the system operators before the day-ahead EOM closed. [17] proposed a coordination scheme between the TSO and the DSOs that could allow distributed resources to provide both real and reactive power flexibility, and showed that such coordination could reduce cost and increase system strength against voltage collapse on a test system. [18] tested an operational framework where TSO-DSO coordination can be carried out, while [19] discussed how different active levels of end-users and digitization levels of the distribution power network can result in different possibilities for end-users to provide flexibility services at both the distribution and the transmission levels.

Most of literature on TSO-DSO coordination focuses on the operation strategies of the system operators at the distribution level, which in many cases was simulated on a test system. Some noteworthy exceptions to this trend are [20–22], and [9]. [20] showed how it was possible operationally for end-users to contribute to the flexibility required at both the TSO and DSO level due to the uncertainty of VRE power output with a Building-to-grid (BtG) integration framework, replacing some traditional reserve scheduling services without jeopardizing the stability of the grid or violating thermal comfort constraints of buildings. [21] provided field demonstrations for TSO-DSO-Customer coordination in real world local flexibility markets, which successfully alleviated network congestion, reduce system costs while keeping a secure operation. It also highlighted engagement among stakeholders, customer-friendly technical requirements, and timing of the market as key factors for the success of local flexibility markets. Both [9,22] showed the potential value of coordination between DSOs and TSOs at a national level. [22] showed that DR programs, distributed storage and other DERs together provided reduced total costs of the system by 1%, half of which resulted from reduced number of start-ups and shutdowns of conventional power plants. [9] showed that TSO-DSO coordination for redispatch could become valuable in a renewable energy dominated power system, saving up to 300 million Euros in Germany in 2030. Nevertheless, to the best of our knowledge there is a gap in the literature where a multi-level coordination between the TSO, the DSOs, and the end-users is studied thoroughly. This was also noted and observed in [23,24]. All in all, the work developed in this paper has the following contributions to the literature:

- Developed multiple power system models that represent the power market and grids. This includes modeling the day-ahead, re-dispatch operations of transmission grid, distribution grids, and end-user flexibility. These models are combined and simulate a flow of decisions of the power system where TSO-DSO scheme plays a central role. The literature has tended to focus on only certain aspects when linking models or taken a single perspective (e.g. the TSO, or DSO only), this has been noted as a current gap in the field [10,25].
- The model and analysis is applied to the entire Norwegian power system. This is country wide representing all power market zones and all the DSOs grids. The large implementation scale in a real-life case study provides a fresh and tangible outlook on the implications of TSO-DSO coordination as noted in [9]. Moreover, the data, models and implementation have been made open source[1].

---

[1] The model and data are available at GitHub: https://github.com/TonyYenTWN/trEnD.

- Implementing multiple models required significant methodological advancements to attain a high level of granularity and accurately represent end-users. For instance, achieving a spatial resolution of 10×10 km involved the development of a Bayesian maximum entropy method to calculate electricity demand across the entire country. These meticulous details in crafting the representation of the countrywide power system establish a robust framework that can be applied to replicate TSO-DSO schemes in other countries or settings.
- The paper adopts an end-user perspective as a central element to comprehensively assess the impact of their participation in power markets with TSO-DSO schemes. Unlike much of the existing literature, which predominantly focuses on mid-size distributed energy sources, this study places significant emphasis on analyzing the intricacies and dynamics of end-user and EVs contributions to grid operations.

For a comprehensive summary of the key findings of the relevant literature, readers may refer to Table 8 in Appendix A.

3. Modeling framework

3.1. Scenarios of TSO-DSO coordination

To study the effects of allowing end-users to participate in power markets with TSO-DSO coordination, we propose a simple TSO-DSO coordination scheme that allows us to capture these effect in the model: while the market clearing in the EOM remains the same as status quo, the TSO will be able to consider flexibility resources on the distribution power network during redispatch. To ensure that the activation of these distributed flexible resources will not violate physical constraints on the distribution power networks, DSOs will validate whether the distributed flexible resources can be considered in the redispatch once the market clears in the EOM. Only the bids allowed by the DSOs can then be considered during redispatch by the TSO.

In essence, our TSO-DSO coordination scheme corresponds to a framework with a single, short-term, transmission level congestion management sub-market as described in [26], if one considers the redispatch process (further described in Section 3.5.2) as a sub-market. We do not consider the validation process from the DSOs as a separate sub-market since there is no monetary flow during it. However, since the DSOs validate the submitted bids by checking whether constraints are honored in an extreme operational condition (see Section 3.4.2), this means that distributed flexibility resources are implicitly prioritized for local grid management. We choose this simple framework that guarantees secure system operation at the expense of economic efficiency as an optimal but more sophisticated coordination scheme is not necessary to study the effects of end-users participation in the market. The lack of advance resource allocation for the flexibility needed at transmission and distribution level is of course a limitation of the study.

With this TSO-DSO coordination scheme, we simulate the power market and power network of Norway under 3 scenarios:

1. Reference: in this scenario there is no TSO-DSO coordination, and end-users do not provide flexibility services to the power network. Other distributed flexible resources enter redispatch without security validation from DSOs. This is the scenario that is closest to the status quo in Norway.
2. Partially Flexible: in this scenario there is TSO-DSO coordination. Some end-users, along with other distributed flexible resources, enter redispatch after security validation from DSOs. In this scenario it is assumed that these end-users can only provide flexibility in redispatch, while their electricity demand profiles in the EOM remain the same as in the reference scenario.

Table 1

The features of the flexibility assets considered. For smart appliances, the proportion relative to the default electricity demand is shown.

End-user type	Smart appliance	BESS	EV BESS
Inflexible	0	0 kW/0 kWh	0 kW/0 kWh
Inflexible + EV	0	0 kW/0 kWh	2 kW/8 kWh
Active	0.1	1 kW/10 kWh	2 kW/8 kWh

Table 2

Relative proportion of end-user types under different scenarios.

	Reference	Partially Flexible	Fully Flexible
Inflexible	90%	90%	90%
Inflexible + EV	10%	10%	5%
Active	0%	0%	5%

3. Fully Flexible: in this scenario there is TSO-DSO coordination. The TSO-DSO coordination scheme in this scenario is the same as that in the Partially Flexible Scenario. As in the Partially Flexible Scenario, some end-users, along with other distributed flexible resources, enter redispatch after security validation from DSOs. However, as opposed to the Partially Flexible Scenario, the end-users can now provide flexibility both in redispatch and in the EOM by changing their electricity demand profiles in the EOM.

The comparison between the Reference Scenario and the Partially Flexible scenario allows us to investigate the impacts of allowing end-users to provide flexibility in redispatch only (without affecting their electricity demand profile in the EOM), and the comparison between Partially and Fully flexible scenarios allows us to investigate the impacts of allowing end-users to also change their electricity demand profile in the EOM.

A schematic chart of the sequence of actions under the three scenarios can be seen in Fig. 1. As illustrated on the figure, TSO-DSO coordination in the Partially and Fully Flexible Scenarios is accomplished by adding a DSO filtering step after the EOM clearing and before the TSO solve the redispatch problem. The coordination scheme is therefore embedded in an existing market framework, with one sub-market for congestion management at the transmission level.

3.2. Modeling end-users

3.2.1. Different types of end-users

To investigate how different types of end-users will be affected under the scenarios, end-users at each spatial point are categorized as:

1. Inflexible end-users: these end-users do not possess any flexibility assets. They represent the majority of the end-users today.
2. Inflexible end-users with EV: these end-users possess home-charging EV, but they do not actively provide their flexibility even if they are allowed to do so.
3. Active end-users: in addition to home-charging EV, these end-users possess flexibility investments such as smart appliance and battery energy storage systems (BESS), and also actively provide their flexibility in the EOM or for redispatch when allowed.

A comparison between the inflexible end-users with and without EV provides insights into the default impacts of the flexibility assets the end-users possess to their electricity prices. The active end-users bring insights to the additional values from the flexibility assets by providing flexibility in the EOM and redispatch, whenever possible.

The flexibility features of the three types of end-users is categorized in Table 1, and their relative proportion at each spatial point under the scenarios is shown in Table 2. The storage capacity of the BESS is based on industrial recommendations for end-users [27,28]. The storage capacity of EV BESS is set to 8 kWh to be able to cover the daily average
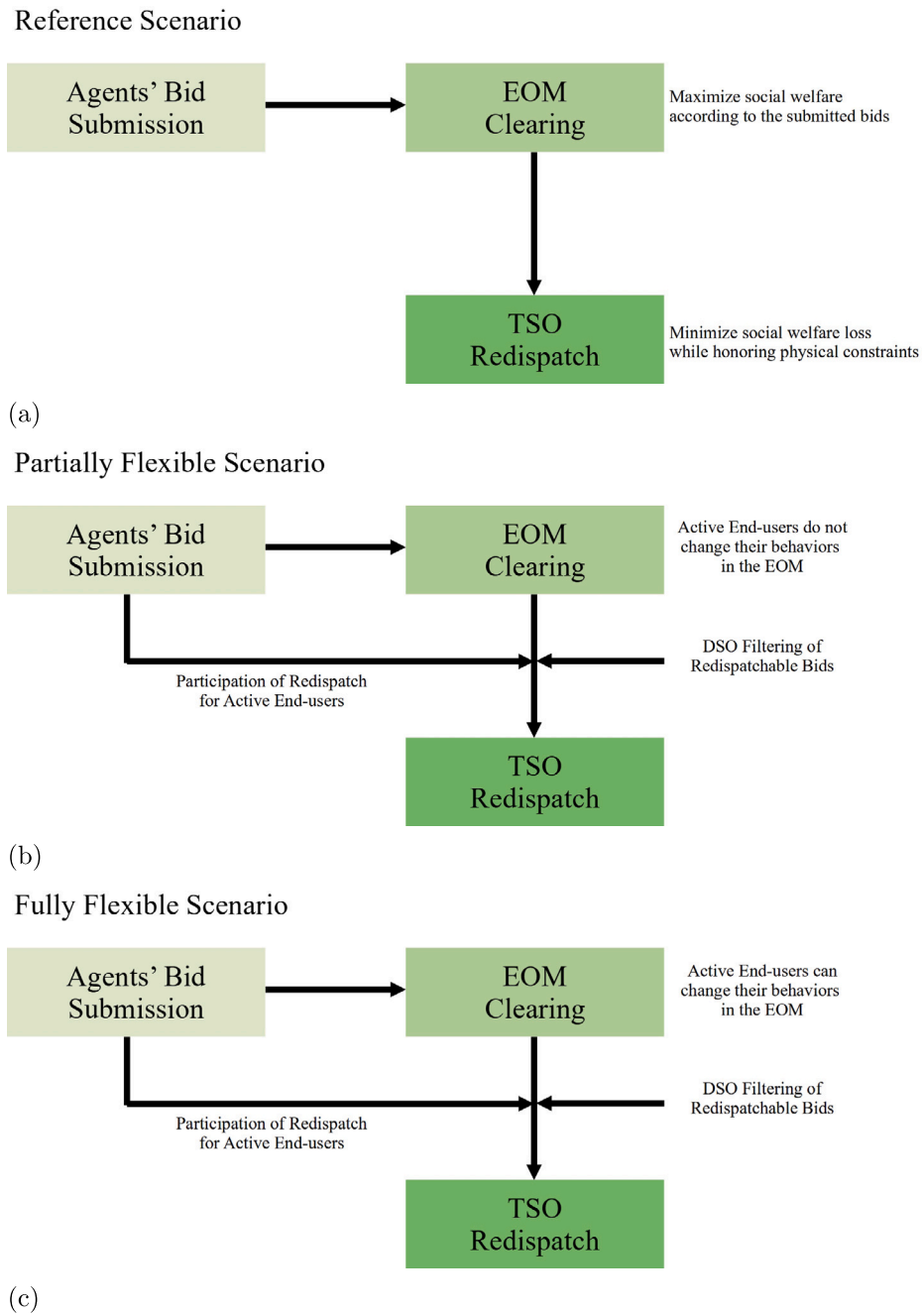
Reference Scenario

(a)

Partially Flexible Scenario

(b)

Fully Flexible Scenario

(c)

Fig. 1. Schematic chart of the sequence of actions in the modeled Norwegian power market under different scenarios.

electric demand per capita for EVs. This value is estimated based on the annual energy consumption from petroleum in the Norwegian transport sector [29]. Acknowledging that this is an conservative constraint on the storage capacity, we conduct an additional analysis by increasing the storage capacity of EV BESS threefold to 24 kWh to reflect their potential to provide more flexibility in Section 4. The proportion of active end-users is chosen to both represent the early stage of the transition in the types of end-users while also allow their collective impacts to be observable in the model.

3.2.2. Electricity demand profiles estimation

To model the interactions between the end-users and the system operators at different levels, electricity demand profiles of the end-users with high spatial resolution and sufficient temporal resolution is needed. Since to the best of our knowledge, there is no such data

available in the public domain for Norway, we have to estimate the profiles based on both hourly electricity demand data in the five power market bidding zones and high-resolution population density data of Norway (see Appendix A for detailed methodology developed to estimate the profiles). As a result, we obtain the electricity demand profiles of the end-users with a 10 km × 10 km spatial resolution (shown in Fig. 2).

3.2.3. Operational behaviors of end-users

Similar to [30,31], the operational behavior of end-users is modeled via the following utility optimization problem:

$$\max_{U_i^s(t),\, U_i^d(t)} \sum_{t \in \mathcal{T}_i} M^s(x,t)U_i^s(t) - M^d(x,t)U_i^d(t) \ \forall\, i \in \{E\}(x), x. \tag{1}$$
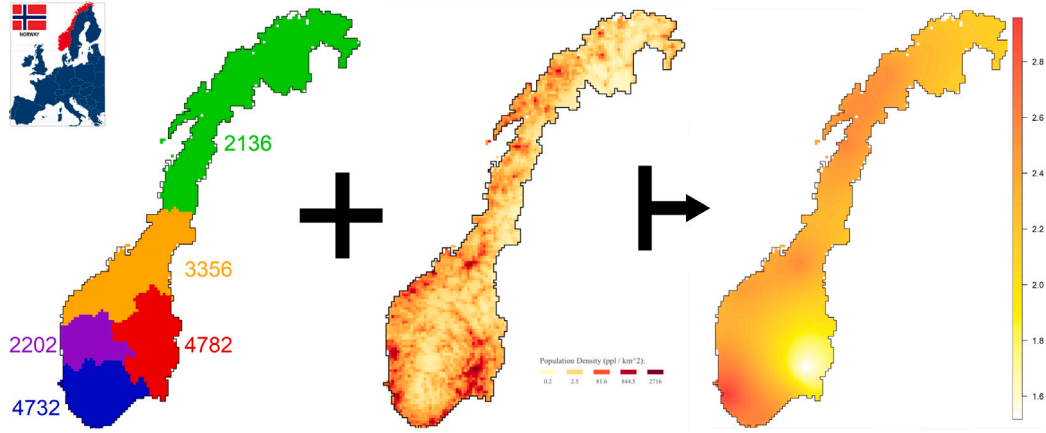
Fig. 2. Schematic chart of how the electricity demand profiles of the end-users are estimated. Left: electricity demand (MWh) of a hour in the bidding zones of Norway. Center: population density (ppl/km²) of Norway. Right: estimated electricity demand per capita (kWh/ppl).

Here $\mathcal{T}_i$ is the foresight time interval of the end-user i, $M^s(x,t)$ and $M^d(x,t)$ the expected procurement (retailer) price for electricity production (demand) at spatial point x and time t, $U_i^s(t)$ and $U_i^d(t)$ the scheduled production (demand) quantity of end-user i whose values they must decide upon, and $\{E\}(x)$ the set of end-users at spatial point x. Note that all the notations for parameters and variables are described in Table 9 (see Appendix). Other important assumptions to consider:

1. The expected procurement (retailer) price for electricity production (demand) is assumed to be the same as the expected market clearing price in the EOM, which is calculated by using the merit order curves (see Section 3.3) and electricity demand data (see Section 3.7). The demand is assumed to be inflexible when calculating the expected market clearing prices.

2. For each spatial point, the 3 types of end-users indicated in Section 3.2.1 are considered in $\{E\}(x)$, and the individual end-users are assumed to be homogeneous, with flexibility features described in Table 1. At each spatial point, the relative proportion of different types of end-users is the same, as indicated in Table 2. The optimization problem described in Eq. (1) is optimized for each type of end-users at each spatial point at the beginning of $\mathcal{T}_i$, although only the active end-users will have a non-trivial feasible space for the decision variables that actually requires computational effort to obtain a solution (for other types of end-users $U_i^s(t)$ will always be 0 and $U_i^d(t)$ will always be their inflexible electricity demand).

Eq. (1) is subject to an equality constraint representing the balancing of demand and supply for end-user i at time t:

$$U_i^d(t) - U_i^s(t) = D_{0,i}(t) + U_i^b(t) + U_i^{ev}(t) + U_i^{sa}(t) \;\forall\, i, t. \tag{2}$$

Here $D_{0,i}(t)$ is the inflexible electricity demand of end-user i at time t, $U_i^b(t)$, $U_i^{ev}(t)$, and $U_i^{sa}(t)$ the electricity produced (consumed) from the BESS, home-charging EV, and smart appliance owned by end-user i at time t.

For BESS, there are the following equality constraints representing the law of energy conservation:

$$U_i^b(t) = \frac{1}{\eta_i^{ch,b}} ch_i^b(t) - \eta_i^{dc,b} dc_i^b(t) \;\forall\, i, t, \tag{3}$$

$$soc_i^b(t) = soc_i^b(t-1) + ch_i^b(t) - dc_i^b(t) \;\forall\, i, t. \tag{4}$$

Here $\eta_i^{ch,b}$ and $\eta_i^{dc,b}$ are the charge (discharge) efficiency for the BESS owned by end-user i, $ch_i^b(t)$ and $dc_i^b(t)$ the charge (discharge) volume of the BESS, and $soc_i^b(t)$ the state of charge (SOC) of the BESS.

For home-charging EV, the equality constraints representing the law of energy conservation are almost identical to Eq. (3) and Eq. (4)

$$U_i^{ev}(t) = \frac{1}{\eta_i^{ch,ev}} ch_i^{ev}(t) - \eta_i^{dc,ev} dc_i^{ev}(t) \;\forall\, i, t, \tag{5}$$

$$soc_i^{ev}(t) = soc_i^{ev}(t-1) + ch_i^{ev}(t) - dc_i^{ev}(t) - d_i^{ev}(t) \;\forall\, i, t. \tag{6}$$

Here $\eta_i^{ch,ev}$ and $\eta_i^{dc,ev}$ are the charge (discharge) efficiency for the EV owned by end-user i, $ch_i^{ev}(t)$ and $dc_i^{ev}(t)$ the charge (discharge) volume of the EV, $soc_i^{ev}(t)$ the state of charge of the EV, and $d_i^{ev}(t)$ the electricity consumed for providing transportation service of the EV.

For smart appliances, assuming that their total electricity demand is constant over $\mathcal{T}_i$, the following equality constraints should hold:

$$\sum_{\tau \in \mathcal{T}_i \oplus [-\Delta t, 0]} d_i^{sa}(\tau, t) = U_i^{sa}(t) \;\forall\, i, t \in \mathcal{T}_i, \tag{7}$$

$$\sum_{\tau \in \mathcal{T}_i} d_i^{sa}(t, \tau) = d_i^{sa}(t) \;\forall\, i, t \in \mathcal{T}_i \oplus [-\Delta t, 0] \tag{8}$$

Here $d_i^{sa}(t_1, t_2)$ is the flexible demand shifted from t_1 to t_2 via smart appliances by end-user i and Δt the maximum possible time shift, $d_i^{sa}(t)$ the unfulfilled default demand profile of the smart appliances, and $\oplus$ the Minkowski sum operator.

The variables $ch_i^b(t)$, $dc_i^b(t)$, $soc_i^b(t)$, $ch_i^{ev}(t)$, $dc_i^{ev}(t)$, $soc_i^{ev}(t)$, and $d_i^{sa}(t_1, t_2)$ are subject to box constraints in the form of Eq. (9):

$$0 \le ch_i^b(t) \le \overline{ch_i^b}(t) \qquad \forall\, i, t, \tag{9a}$$

$$0 \le dc_i^b(t) \le \overline{dc_i^b}(t) \qquad \forall\, i, t, \tag{9b}$$

$$\underline{soc_i^b}(t) \le soc_i^b(t) \le \overline{soc_i^b}(t) \qquad \forall\, i, t, \tag{9c}$$

$$0 \le ch_i^{ev}(t) \le \overline{ch_i^{ev}}(t) \qquad \forall\, i, t, \tag{9d}$$

$$0 \le dc_i^{ev}(t) \le \overline{dc_i^{ev}}(t) \qquad \forall\, i, t, \tag{9e}$$

$$\underline{soc_i^{ev}}(t) \le soc_i^{ev}(t) \le \overline{soc_i^{ev}}(t) \qquad \forall\, i, t, \tag{9f}$$

$$0 \le d_i^{sa}(t_1, t_2) \le d_i^{sa}(t_1)\, \Pi\left(\frac{t_1 - t_2}{2\Delta t}\right) \qquad \forall\, i, t_1, t_2. \tag{9g}$$

Here an underline indicates the lower bound of a variable and an overline indicates the upper bound of a variable. The lower and upper bounds of $soc_i^b(t)$, $soc_i^{ev}(t)$ are set to 0 for end-users that do not possess BESS or EV. For $ch_i^{ev}(t)$ and $dc_i^{ev}(t)$, the upper bounds also depend on the whether the EV is under idle mode at home at time t; the upper bounds of these values are set to 0 if the EV is not at home. $\Pi(\cdot)$ is the rectangle function.

Once the optimal scheduled production (demand) is determined, the end-users bid accordingly in the EOM. The bids of the inflexible end-users are modeled as inflexible demand, i.e. they bid with the highest possible price when entering the EOM. The bids of the active end-users are decomposed into an inflexible part and a flexible part. They bid with the highest possible price for the inflexible demand part and with the expected market clearing price for the flexible part.

3.3. Other participants in the power market

The model currently includes hydro power plants and onshore wind power plants in Norway. We generate a normalized merit order curve for each bidding zone based on the actual EOM price and residual demand data and assume that all hydro power plants in that bidding zone bid according to the curve.

For onshore wind power plants, we estimate the capacity factor field of the technology with the same methodology as in Section 3.2.2 with wind power output and capacity data from each bidding zones. The capacity factor field is constructed so that the aggregated wind power output of a bidding zone matches the actual data. The onshore wind power plants are modeled as inflexible supply and will submit bids with the lowest possible price when entering the EOM.

In order to prevent load-shedding from inflexible demand due to the constraints in the power network, we also added some slack gas power plants at each spatial point in the model.[2] The marginal operation cost of these power plants are sufficiently high so they will not be able to enter the EOM, but will be activated during redispatch whenever there are no other available flexible resources at a certain node in the power network.

3.4. Distribution power network

3.4.1. Power flow modeling

The power network data described in Section 3.7 contains 126,435 power lines, almost all of which at the distribution level. While it might be possible to model the distribution power networks exactly with all these power lines, for the scope of this paper there is no need to represent the distribution power networks with a spatial resolution greater than that of the electricity demand profiles of the end-users. Instead, a stylized model for the distribution power networks is adopted based on some statistical features of the power lines; the spatial resolution of this stylized model corresponds to the regional distribution power networks [32] in the Norwegian context. See Appendix B for more details on the model.

3.4.2. Optimization

In scenarios where TSO-DSO coordination exists and DSOs are tasked to filter submitted supply and demand bids of market participants within their responsible distribution power network during the redispatch step, the DSOs will run 2 optimal DC power flow problems, one for the supply bids and the other for the demand bids, to determine the merit order curves of supply and demand bids eligible for entering the redispatch scheduling of the TSO. The optimal DC power flow problem for a DSO to determine eligible supply bids for entering the redispatch scheduling of the TSO is

$$\max_{\hat{Q}_j^s(t)} \sum_{i \in \{A\}_{\mathbb{D}}} \sum_{j \in \{\mathbb{B}\}_i} \left(B^{\max} - \hat{B}_j^s(t) \right) \hat{Q}_j^s(t) \, \forall \, \mathbb{D}, t. \tag{10}$$

Here $\{A\}_{\mathbb{D}}$ is the set of all the market participants in the operational area of a particular DSO $\mathbb{D}$. $\{\mathbb{B}\}_i$ is the set of bids submitted by a particular market participant i. $B^{\max}$ is the maximum bidding price in the EOM. $\hat{B}_j^s(t)$ is the equivalent bidding price of supply bid j considered in the DSO problem. $\hat{Q}_j^s(t)$ is the quantity of supply bid j allowed to enter the redispatch problem of the TSO at time t, whose value the DSOs must decide upon.

Eq. (10) is subject to the following equality constraints representing the physics in the distribution power network: Eq. (11) is the governing

equation relating phase angles and DC power flow, while Eq. (12) is the power flow equation for DC power flow problems.

$$[\mathcal{Y}]_{\mathbb{D}}[\mathcal{I}]_{\mathbb{D}}^{\mathrm{T}}\{\theta\}_{\mathbb{D}}(t) = \{I\}_{\mathbb{D}}(t) \, \forall \, \mathbb{D}, t, \tag{11}$$

$$[Y]_{\mathbb{D}}\{\theta\}_{\mathbb{D}}(t) = \{S\}_{\mathbb{D}}(t) \, \forall \, \mathbb{D}, t. \tag{12}$$

Here $[\mathcal{Y}]_{\mathbb{D}}$ is the line admittance matrix of the distribution power network in the operation area of a particular DSO $\mathbb{D}$, $[\mathcal{I}]_{\mathbb{D}}$ the signed incidence matrix of the network, $\{\theta\}_{\mathbb{D}}(t)$ the phase angles at the nodes of the network at time t, $\{I\}_{\mathbb{D}}(t)$ the DC power flow on the power lines of the network at time t, $[Y]_{\mathbb{D}}$ the nodal admittance matrix of the network, and $\{S\}_{\mathbb{D}}(t)$ the power source (sink) at the nodes of the network at time t. Note that $[Y]_{\mathbb{D}} = [\mathcal{I}]_{\mathbb{D}}[\mathcal{Y}]_{\mathbb{D}}[\mathcal{I}]_{\mathbb{D}}^{\mathrm{T}} + [\mathcal{Y}_{sh}]_{\mathbb{D}}$, where $[\mathcal{Y}_{sh}]_{\mathbb{D}}$ is the shunt admittance matrix of the nodes in $\mathbb{D}$.

Eq. (10) is also subject to equality constraints in the form of Eq. (13), linking the decision variables $\hat{Q}_j^s(t)$ with the physical variables $\{S\}_{\mathbb{D}}(t)$.

$$\sum_{i \in \{A\}_n} \sum_{j \in \{\mathbb{B}\}_i} \hat{Q}_j^s(t) = S_n(t) \, \forall \, \mathbb{D}, \, n \in \{\mathbf{N}\}_{\mathbb{D}}, t. \tag{13}$$

Here $\{\mathbf{N}\}_{\mathbb{D}}$ is the set of nodes in the DSO $\mathbb{D}$, $\{A\}_n$ the market participants at node n, and $S_n(t)$ the power source at the node n at time t.

The variables $\hat{Q}_j^s(t)$, $\{\theta\}_{\mathbb{D}}(t)$, $\{I\}_{\mathbb{D}}(t)$, and $\{S\}_{\mathbb{D}}(t)$ are subject to box constraints in the form of Eq. (14).

$$0 \le \hat{Q}_j^s(t) \le \overline{Q_j^s}(t) \qquad \forall \, j, t, \tag{14a}$$

$$\underline{\{\theta\}_{\mathbb{D}}}(t) \le \{\theta\}_{\mathbb{D}}(t) \le \overline{\{\theta\}_{\mathbb{D}}}(t) \qquad \forall \, \mathbb{D}, t, \tag{14b}$$

$$\underline{\{I\}_{\mathbb{D}}}(t) \le \{I\}_{\mathbb{D}}(t) \le \overline{\{I\}_{\mathbb{D}}}(t) \qquad \forall \, \mathbb{D}, t, \tag{14c}$$

$$-\infty < S_n(t) \le 0 \qquad \forall \, \mathbb{D}, \, n \in \{\mathbf{T}\}_{\mathbb{D}}, t. \tag{14d}$$

Here an underline below indicates the lower bound of a variable and a bar above indicates the upper bound of a variable (for example, $\overline{Q_j^s}(t)$ is the submitted quantity of bid j). $\{\mathbf{T}\}_{\mathbb{D}}$ is the set of nodes that connect to the transmission power network in $\mathbb{D}$. In order to have non-trivial solutions for Eq. (10), we model the nodes in $\mathbb{D}$ which link to the transmission power network as current sinks with no upper limit on the power drawn from the distribution power network.

By solving the optimization problem described with Eq. (10) to Eq. (14), DSOs consider the extreme case where all the validated supply are activated and only the connection node to the transmission power network draws power from the rest of the distribution power network. This ensures that when the TSO actually activates the validated supply bids, they will not result in voltage or power flow violations on the distribution power networks.

Similarly, the optimal DC power flow problem for a DSO to determine eligible demand bids for entering the redispatch problem of the TSO is

$$\max_{\hat{Q}_j^d(t)} \sum_{i \in \{A\}_{\mathbb{D}}} \sum_{j \in \{\mathbb{B}\}_i} \hat{B}_j^d(t)\hat{Q}_j^d(t) \, \forall \, \mathbb{D}, t. \tag{15}$$

The equality constraints the DSO needs to consider when solving Eq. (15) are also Eq. (11), Eq. (12), and Eq. (13), and the box constraints are similar to that of Eq. (14). The main differences are that $\hat{Q}_j^s(t)$ ($\overline{Q_j^s}(t)$) are now replaced with $\hat{Q}_j^d(t)$ ($\overline{Q_j^d}(t)$) (the only exceptions are the slack gas power plants, which are kept in the optimal DC power flow problem so that inflexible demand will not be curtailed), and that $S_n(t)$ now lies in $[0, \infty)$ for $n \in \{\mathbf{T}\}_{\mathbb{D}}$.

3.5. Power market and transmission system operator

3.5.1. Internationally-coupled market clearing of wholesale electricity

The wholesale power market of Norway is embedded in Nordpool, a pan-European electricity exchange platform that allows participants in Norway to trade electricity with their counterparts in the neighboring

---

[2] The slack power plants are added to avoid model infeasibility. We assume the techno-economic parameters of these power plants are those of gas power plants, because in practice the majority of Norway's few thermal power plants are such. Of course, other flexibility supply options can be considered.

countries in a day-ahead EOM. Any model regarding the economic dispatch scheduling at the transmission power network level in Norway must therefore also take into account cross-border flows resulted due to the exchange.

In our model, there exists an international market operator (IMO) which plays the role of Nordpool and conducts market clearing of the internationally-coupled EOM. The market clearing is performed by solving an economic surplus maximization problem given by Eq. (16),

$$\max_{Q_j^d(t), Q_j^s(t)} \sum_{z \in \{Z\}} \sum_{i \in \{A\}_z} \sum_{j \in \{\mathbb{B}\}_i} \left(B_j^d(t) Q_j^d(t) - B_j^s(t) Q_j^s(t) \right) \forall t. \tag{16}$$

Here $\{Z\}$ is the set of bidding zones involved in the internationally-coupled EOM. $\{A\}_z$ is the set of all the market participants in bidding zone z. $B_j^d(t)$ and $B_j^s(t)$ are the participant-determined bidding price of demand (supply) of bid j at time t. $Q_j^d(t)$ and $Q_j^s(t)$ are the cleared bidding quantity of demand (supply) of bid j at time t in the EOM, whose values the IMO must decide upon.

The economic surplus maximization problem for the IMO is subject to equality constraints in the form of Eq. (17), representing the law of energy conservation for each bidding zones involved.

$$\left(\sum_{i \in \{A\}_z} \sum_{j \in \{B\}_i} Q_j^d(t) - Q_j^s(t) \right) + \sum_{\zeta \in \{Z\}} F_{z\zeta}(t) = 0 \,\forall z, t. \tag{17}$$

Here $F_{z\zeta}(t)$ is the cross-border flow from bidding zone z to bidding zone ζ at time t, which is antisymmetric by construction (i.e. $F_{z\zeta}(t) = -F_{\zeta z}(t)$).

The variables $Q_j^d(t)$, $Q_j^s(t)$, and $F_{z\zeta}$ are subject to box constraints in the form of Eq. (18), restricting them to physically-meaningful values.

$$0 \leq \quad Q_j^d(t) \leq \quad \overline{Q_j^d}(t) \quad \forall j, t, \tag{18a}$$

$$0 \leq \quad Q_j^s(t) \leq \quad \overline{Q_j^s}(t) \quad \forall j, t, \tag{18b}$$

$$\underline{F_{z\zeta}}(t) \leq \quad F_{z\zeta}(t) \leq \quad \overline{F_{z\zeta}}(t) \quad \forall z, \zeta, t. \tag{18c}$$

Here an underline indicates the lower bound of a variable and an overline indicates the upper bound of a variable.

Once the IMO solves Eq. (16) for a specific time slice t, the values of the cross-border flows $F_{z\zeta}(t)$ will be passed on to the TSO as boundary conditions when it solves the optimal power flow problem for its redispatch scheduling. The resulting market clearing prices at each bidding zones will also be stored for calculations in the settlement part of the model.

It should be noted that in the actual Norwegian power market, after the day-ahead EOM is cleared and before the TSO carries out the redispatch, market participants can trade with each other in the intraday EOM to change their supply/demand schedule whenever necessary. In our model, we simplify the multistage process of energy-only trades into one single stylized EOM that occurs just before redispatch, representing the final resulting schedule in all the EOMs in real life. The simplification of multistage energy trades into a stylized EOM neglects the process of increasing information and decreasing uncertainty/flexibility as the system approaches from day-ahead to real time.

3.5.2. Redispatch of the TSO

The market clearing result in Section 3.5.1 does not consider the network constraints within each bidding zone. To ensure that the supply and demand schedules honor the physical constraints of the transmission power network, the TSO of the modeled bidding zones will determine the redispatch scheduling of bids submitted into the EOM.

To this end, the TSO will solve an optimal power flow problem that has a similar objective function as that in Eq. (16), with the only difference that $\{Z\}$ now only covers bidding zones that are within the control area of the TSO:

$$\max_{\tilde{Q}_j^d(t), \tilde{Q}_j^s(t)} \sum_{z \in \{Z\}} \sum_{i \in \{A\}_z} \sum_{j \in \{\mathbb{B}\}_i} \left(B_j^d(t) \tilde{Q}_j^d(t) - B_j^s(t) \tilde{Q}_j^s(t) \right) \forall t. \tag{19}$$

Here $\tilde{Q}_j^d(t)$ and $\tilde{Q}_j^s(t)$ are the confirmed bidding quantity of demand (supply) of bid j at time t that the TSO must decide upon during redispatch scheduling.

The constraints for this optimal power flow problem are almost identical to the ones we encountered in Section 3.4.2, namely

$$[\mathcal{Y}]_{\mathbb{T}} [\mathcal{I}]_{\mathbb{T}}^{\mathrm{T}} \{\theta\}_{\mathbb{T}}(t) = \{I\}_{\mathbb{T}}(t) \,\forall t, \tag{20}$$

$$[Y]_{\mathbb{T}} \{\theta\}_{\mathbb{T}}(t) = \{S\}_{\mathbb{T}}(t), \tag{21}$$

$$\sum_{i \in \{A\}_n} \sum_{j \in \{\mathbb{B}\}_i} \tilde{Q}_j^s(t) - \tilde{Q}_j^d(t) = S_n(t) + \partial S_n(t) \,\forall n \in \{\mathbf{N}\}_{\mathbb{T}}, t. \tag{22}$$

Here the notation is almost equivalent to those in Eq. (11), Eq. (12), and Eq. (13), with the major difference being that we now consider variables within in the control area of the TSO (denoted as $\mathbb{T}$). As mentioned in Section 3.5.1, cross bordered flows obtained in the market clearing by the IMO are boundary conditions the TSO needs to take into account when solving its optimal power flow problem, which is denoted as $\partial S_n(t)$ here.

The variables $\tilde{Q}_j^s(t)$, $\tilde{Q}_j^d(t)$, $\{\theta\}_{\mathbb{T}}(t)$, $\{I\}_{\mathbb{T}}(t)$, and $\{S\}_{\mathbb{T}}(t)$ are subject to box constraints in the form of Eq. (23).

$$0 \leq \quad \tilde{Q}_j^s(t) \leq \quad \hat{Q}_j^s(t) \text{ or } \overline{Q_j^s}(t) \quad \forall j, t, \tag{23a}$$

$$0 \leq \quad \tilde{Q}_j^d(t) \leq \quad \hat{Q}_j^d(t) \text{ or } \overline{Q_j^d}(t) \quad \forall j, t, \tag{23b}$$

$$\underline{\{\theta\}_{\mathbb{T}}}(t) \leq \quad \{\theta\}_{\mathbb{T}}(t) \leq \quad \overline{\{\theta\}_{\mathbb{T}}}(t) \quad \forall t, \tag{23c}$$

$$\underline{\{I\}_{\mathbb{T}}}(t) \leq \quad \{I\}_{\mathbb{T}}(t) \leq \quad \overline{\{I\}_{\mathbb{T}}}(t) \quad \forall t. \tag{23d}$$

Note that $\tilde{Q}_j^s(t)$ ($\tilde{Q}_j^d(t)$) is constrained by either $\hat{Q}_j^s(t)$ ($\hat{Q}_j^d(t)$) or $\overline{Q_j^s}(t)$ ($\overline{Q_j^d}(t)$), depending on whether or not TSO-DSO coordination exists.

Note that in practice, redispatch is carried out during the activation of the tertiary control reserve in Norway, but in this model it is simplified to be an adjustment to the EOM results. The implicit assumption behind this simplification is that for market participants, the difference between the bidding price and the market clearing price of a bid in the EOM reflects their opportunity cost of redispatching that bid, and therefore the market participants will bid accordingly in the tertiary control reserve market. This is a direct result from the simplification of multistage energy trades into a stylized EOM described in Section 3.5.1. In reality, opportunity costs will usually increase for market participants as the system approaches real time due to decreasing flexibility, which will affect the bidding quantity and prices market participants can provide during redispatch.

In addition, to guarantee that the redispatch results of the simulation are indeed physically feasible and do not cause voltage collapse, we run an AC power flow model (based on the methodology described in [33]) on the results for validation. For the AC power flow model, we assume that nodes on the transmission power network that are connected directly with hydro-electricity power plants are PU buses whose reference voltage magnitude is 1 per-unit.

3.6. Workflow of the model

The model used in this paper contains a simulation part and a settlement part. In the simulation part, the operation of the power market in Norway is modeled. In each time slice of the simulation, the following steps are conducted:

1. Bid-submission step: in this step, the market participants submit their bids to the IMO of the EOM with strategies described in Section 3.2.3 and Section 3.3.
2. Market clearing step: in this step, all the submitted supply and demand bids are sent to the IMO where an economic surplus maximization problem is conducted (see Section 3.5.1), leading to the market clearing result.

Table 3
Cost in EOM (in million EUR), redispatch cost (in million EUR), and total cost (in million EUR) in the scenarios between (a) winter weeks and (b) summer weeks.

(a)	Reference	Partially Flexible	Fully Flexible		(b)	Reference	Partially Flexible	Fully Flexible
Cost in EOM	262.945	262.945	267.927		Cost in EOM	96.245	96.245	96.036
Redispatch Cost	42.021	41.785	36.438		Redispatch Cost	53.684	53.588	53.888
Total Cost	304.966	304.730	304.365		Total Cost	149.928	149.833	149.924

3. Redispatch step: in this step, the market clearing result from the previous step is adjusted according to the physical constraints of the power networks. In scenarios where TSO-DSO coordination exists, DSOs will filter the submitted bids within their respective operational area (see Section 3.4.2) before the TSO performs the redispatch scheduling (see Section 3.5.2).

4. State update step: in this step, market participants update their relevant states (e.g. the SOC of BESS or the unfulfilled demand of smart appliances). Then the simulation moves on to the next time slice and start from the bid-submission step altogether.

We choose two weeks in winter (01 Jan–14 Jan 2021) and two weeks in summer (01 Jul–14 Jul 2021) as the time periods of our simulation and carry out the steps above consecutively. These two time periods are chosen to represent two extreme operational conditions in the power system in Norway - one with high electricity demand (the winter weeks) and the other with high electricity supply surplus (the summer weeks).

In the settlement part, we define any value exchange between the agents in the considered system (market participants and system operators in Norway) to be the price of a service, and any value generated (lost) endogenously or during exchange with agents outside the system to be the utility (cost) of a service. With this definition we calculate different economic metrics from both the viewpoints of market participants and the entire system.

From the viewpoint of the entire system, we calculate the cost incurred in the EOM and during redispatch scheduling. From the viewpoints of the market participants, the cost of providing energy and flexibility services and the price of obtaining those services are calculated. In particular, the redispatch price is calculated by dividing redispatch compensation by electricity demand for each bidding zone. The redispatch compensation for market participants is assumed to be their opportunity cost to provide redispatch as described in Section 3.5.2.

3.7. Data collection

3.7.1. Power market data

Power market data include actual electricity demand, generation, cross-border flows, and day-ahead electricity prices. Most of the data come from ENTSO-E transparency platform [34], with the exception of those from Great Britain (which come from Elexon portal [35]). Data with higher temporal resolution are assimilated into a resolution of 1 sample per hour by averaging multiple sampling points within hourly intervals.

3.7.2. Power network data

The power network data used in our model come from the Norwegian water resources and energy directorate (NVE) [36]. The geographic information system data from NVE contains line segments representing the power lines in the power network. We cluster the line segments with voltage higher or equal to 132 kV into a single component graph for the transmission power network model. The line segments with lower voltage are used to extract the parameters ρ_N and α in Appendix B.

4. Results and analysis

4.1. System costs

In this section, we discuss the impacts of active end-users from the system's perspective, namely how they affect the operational cost of the power system and the market prices. Table 3 shows the operational cost of the modeled power system for different scenarios. As described in Section 3.6, the operational cost of the power system is divided into the cost incurred in the EOM and during redispatch scheduling. The cost in the EOM represents the operational cost of the power system based on the market clearing results, while the redispatch cost represents the difference in operational cost when redispatch is taken into account. The total cost is the sum of the cost in the EOM and the redispatch cost.

As can be seen, the cost in the EOM in the Reference Scenario and the Partially Flexible Scenario are identical, since active end-users do not change their electricity demand profile in the EOM in the latter scenario (as described in Section 3.1). However, the redispatch cost is reduced in the Partially Flexible Scenario. This cost reduction primarily arises from end-users utilizing their flexibility to replace conventional power plants by providing positive redispatch (increasing generation or decreasing demand in response to local supply deficit) via BESS discharge. As opposed to the Fully Flexible Scenario, the flexibility provided by end-users in the Partially Flexible Scenario is constrained, as they cannot change their electricity demand profile in the EOM. Consequently, they can only balance the SOC of their BESS by providing negative redispatch (decreasing generation or increasing demand in response to local supply surplus) at other time periods. In the Fully Flexible Scenario, by charging (discharging) BESS and EV more in the EOM, end-users can provide more flexibility during positive (negative) redispatch when there is a local deficit (surplus) in supply.

In the winter weeks, active end-users primarily contribute to positive redispatch in response to system needs. Thus, while the redispatch cost decreases in the Fully Flexible Scenario compared with the Partially Flexible Scenario, the cost in the EOM increases. The net effect is a slight decrease in the total cost. Overall, the redispatch cost in the Fully Flexible Scenario is 5.583 million EUR lower than that in the Reference Scenario, whereas the total cost is reduced by 0.601 million EUR.

In the summer weeks, active end-users provide both positive and negative redispatch to a similar extent. The effect of negative redispatch on the system cost is however greater in the Fully Flexible Scenario, and we can see a cost decrease in the EOM while a cost increase in redispatch (compared with the Partially Flexible Scenario). Overall, the Fully Flexible Scenario shows an increase of 0.204 million EUR in redispatch cost compared to the Reference Scenario, whereas the reduction in total cost is 0.004 million EUR. Note that since the charge and discharge strategies of active end-users are set individually and not coordinated among each other (as described in Section 3.2.3), the total system costs do not always improve as a result of more active end-user participation in the power market (as seen here between Partially and Fully Flexible Scenario).

The results of the Fully Flexible Scenario can also be explained by looking at the per capita net redispatch in the simulated periods of the active end-users, illustrated in Fig. 3. As can be seen, in many populated
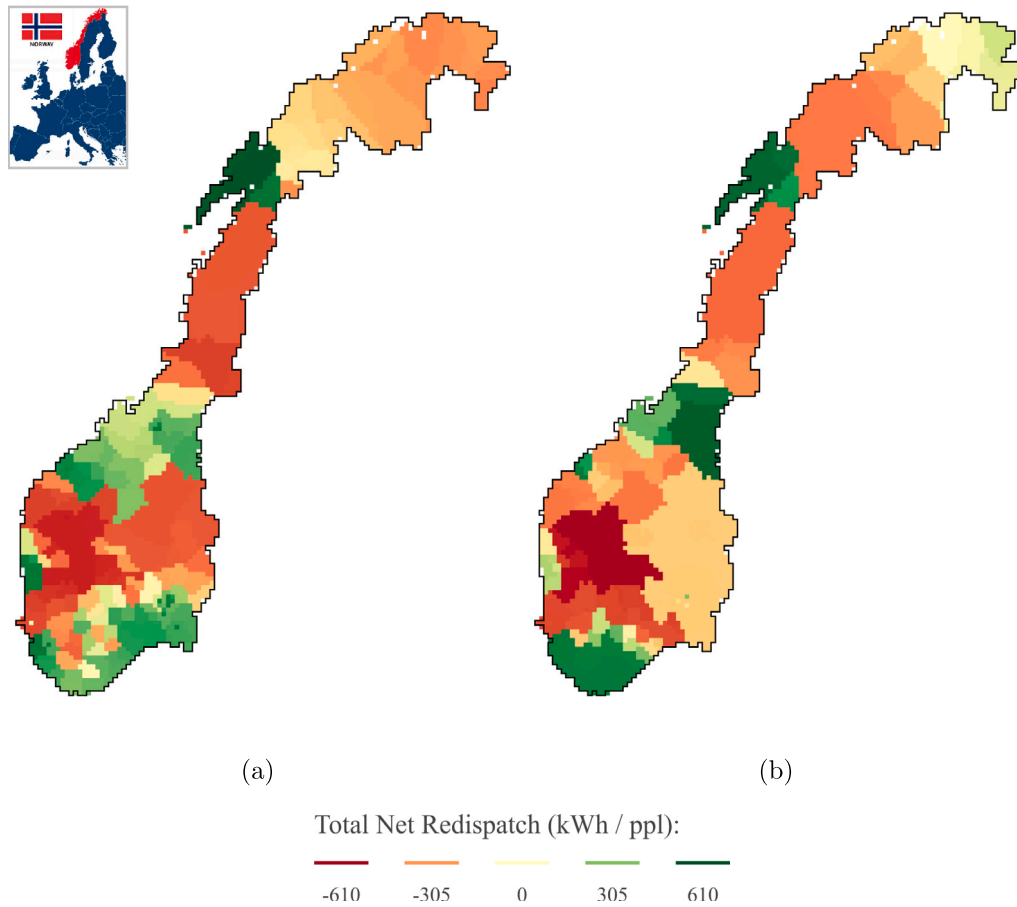
Fig. 3. Per capita net redispatch of the end-users (kWh/ppl) in the Fully Flexible Scenario between (a) Summer weeks and (b) Winter Weeks.

regions in the south of Norway, end-users typically provide positive redispatch on average during the winter weeks and negative redispatch during the summer weeks. The aggregated behaviors of the end-users in these regions dictates how the components in the system cost evolve between the Partially and Fully Flexible Scenarios.

Now, we examine the Fully Flexible Scenario with a less conservative assumption of the storage capacity of EV BESS at 24 kWh (referred to as the 3x EV Scenario hereafter) to investigate the impact of additional flexibility capacity of end-users on the aforementioned results. As seen in Table 4, in the winter weeks, the cost in the EOM increases and the redispatch cost decreases compared with the Partially Flexible Scenario in Table 3, which is consistent with the change between the Partially Flexible Scenario and Fully Flexible Scenario in the same time period, albeit to a greater extent. In the summer weeks, the effect is the opposite: the cost in the EOM decreases and the redispatch cost increases compared with the Partially Flexible Scenario in Table 3. In both time periods, a threefold increase of storage capacity of EV BESS for the active end-users results in the greatest total cost reduction compared with the Reference Scenario. In the winter weeks, this reduction in total cost is around 1 Million EUR, or 0.33% of the total cost in the Reference Scenario; in the summer weeks this reduction is 0.316 Million EUR, or 0.21% of the total cost in the Reference Scenario.

In addition to changing the flexibility features of active end-users, we also explored how the proportion of active end-users would affect their overall impact on the power system. To this end we increased the proportion of end-users with home-charging EVs at each spatial point to 20%, and compared the relevant costs in the winter weeks when all of them are Inflexible + EV end-users and when all of them are

Table 4
Cost in EOM (in million EUR), redispatch cost (in million EUR), and total cost (in million EUR) in the 3x EV Scenario between (a) Winter weeks and (b) Summer weeks.

	Winter weeks	Summer weeks
Cost in EOM	268.042	95.983
Redispatch Cost	35.927	53.628
Total Cost	303.970	149.612

Table 5
Cost in EOM (in million EUR), redispatch cost (in million EUR), and total cost (in million EUR) in the winter weeks for 3x EV Scenario with higher EV share.

	20% Inflexible + EV	20% Active
Cost in EOM	265.654	289.779
Redispatch Cost	41.993	15.910
Total Cost	307.647	305.689

active end-users. As seen in Table 5, the effect of increasing EOM costs and decreasing redispatch costs when more active end-users participate in the power market also exists, but now to a greater extent. The total system cost reduction between 20% Inflexible + EV end-users and 20% active end-users rises to 1.958 Million EUR (a 0.64% reduction), and the redispatch cost reduction rises to 26.083 Million EUR (a 62% reduction).

Table 6
Population density weighted median of average electricity prices (EUR/MWh) for different types of end-users in different bidding zones in scenario 1 between (a) winter weeks and (b) summer weeks.

(a)			(b)		
Zones	Inflexible	Inflexible + EV	Zones	Inflexible	Inflexible + EV
#1	75.9	75.5	#1	73.2	73.8
#2	78.8	78.3	#2	73.7	73.6
#3	49.0	48.7	#3	38.0	37.9
#4	37.0	36.5	#4	28.2	28.0
#5	77.2	77.0	#5	68.8	68.6

Table 7
Population density weighted median of average electricity prices (EUR/MWh) for different types of end-users in different bidding zones in scenario 3 between (a) Winter weeks and (b) Summer weeks.

(a)				(b)			
Zones	Inflexible	Inflexible + EV	Active	Zones	Inflexible	Inflexible + EV	Active
#1	75.8	75.5	62.5	#1	72.9	74.3	64.5
#2	78.8	78.3	66.4	#2	73.6	73.5	63.8
#3	48.9	48.6	42.4	#3	38.0	38.0	32.1
#4	36.6	36.2	32.1	#4	28.0	27.9	24.9
#5	77.3	77.1	68.3	#5	68.4	68.3	58.0

The various 3x EV Scenarios presented here show that the effects of active end-users reported in this section, though small, is consistent under changes of model parameters.

4.2. Average electricity prices among end-users

We now turn our attention to the end-users' perspective, namely the average electricity prices they have to pay during the two simulated time periods. Note that by the definition described in Section 3.6, the electricity price of an end-user is calculated as the sum of what they pay for both wholesale electricity and redispatch services, minus the sum of what they earn from the EOM and redispatch compensation. Their average electricity price is then obtained by dividing their electricity price by their electricity demand (excluding BESS charging) throughout the time period.

Table 6 shows the population density weighted median of average electricity price of different types of end-users in different bidding zones in the Reference Scenario (without TSO-DSO coordination). The spatial heterogeneity of the prices is clear: the average electricity price for end-users in the north of Norway (bidding zones 3 and 4) is much lower than that in the north of Norway (bidding zones 1, 2, and 5). This is the result of both the market clearing prices in the EOM and also the redispatch prices.

Table 7 shows the population density weighted median of average electricity price of different types of end-users in different bidding zones in the Fully Flexible Scenario, with TSO-DSO coordination and active end-users. In the Fully Flexible Scenario, average electricity prices for inflexible end-users remain almost the same as those in the Reference Scenario, while the average electricity prices of the active end-users is in general significantly lower than those of inflexible end-users. This reduction of price is greater in the south of Norway (bidding zones 1, 2, and 5) than in the north of Norway (bidding zones 3 and 4). The greater average electricity price reduction for active end-users in the south of Norway can be explained by Fig. 3, as most of the end-user participation of redispatch occurred in that region.

Note that the observed price reduction for active end-users in Table 7 is primarily attributed to price arbitrage within the Energy Market (EOM) and the avoidance of redispatch costs. However, it is worth considering the potential for additional price reduction by implementing a more supportive price mechanism that allocates all the system cost benefits presented in Table 3 to these active end-users. Indeed, if we redistribute evenly the total cost reduction among the redispatch quantity (positive and negative alike) provided by the active end-users in the Fully Flexible Scenario, the active end-users would receive an additional 3.707 EUR for every MWh of redispatch provided in the winter weeks and 0.032 EUR/MWh in the summer weeks. On average, an active end-user provide 0.451 MWh of redispatch in the winter weeks and 0.360 MWh in the summer weeks, therefore this redistribution will result in a further price reduction of 1.671 EUR in the winter weeks and 0.011 EUR in the summer weeks. As a reference, on average an active end-user has to pay 28.43 EUR for the electricity services in the winter weeks and 16.16 EUR in the summer weeks in the Fully Flexible Scenario.

4.3. Snapshots of tso's and dsos' operations

Fig. 4 shows the average operational conditions of the transmission power network after redispatch in the Reference Scenario in the 2 simulated time periods. As can be seen, in the Reference Scenario, the power network of Norway is more stressed in the winter weeks, especially in the south where the city of Oslo and electricity exports to neighboring nations result in transmission nodes with high electricity demand (marked by red in Fig. 4). Many east–west bound transmission lines in this region are also highly utilized. In the summer weeks, the operation condition is less stressed and the phenomenon described above is less pronounced.

Fig. 5 shows the difference (compared with the Reference Scenario) in the operational conditions of the transmission power network after redispatch in the Fully Flexible Scenario in the winter weeks. While the inclusion of active end-users in redispatch does not significantly affect the average operational condition of the entire simulation period, they do smooth out some of the spatial imbalance between supply and demand during times of peak electricity demand. The inclusion of active end-users in redispatch also smooth out temporal variations of the supply and demand profiles in some DSOs, as shown in Fig. 6; while the effect is not substantial, the inclusion of active end-users in redispatch does smooth out the residual demand (demand minus supply) profiles and the variance of the residual demand decreases in both of the DSOs.

As described in Section 3.5.2, the redispatch results were validated with an AC power flow model and voltage collapse does not occur in the simulated time frame. However, differences in operational conditions in the Reference Scenario and the Fully Flexible Scenario during times of peak electricity demand suggest that system strength against contingency might increase with the participation of active end-users.
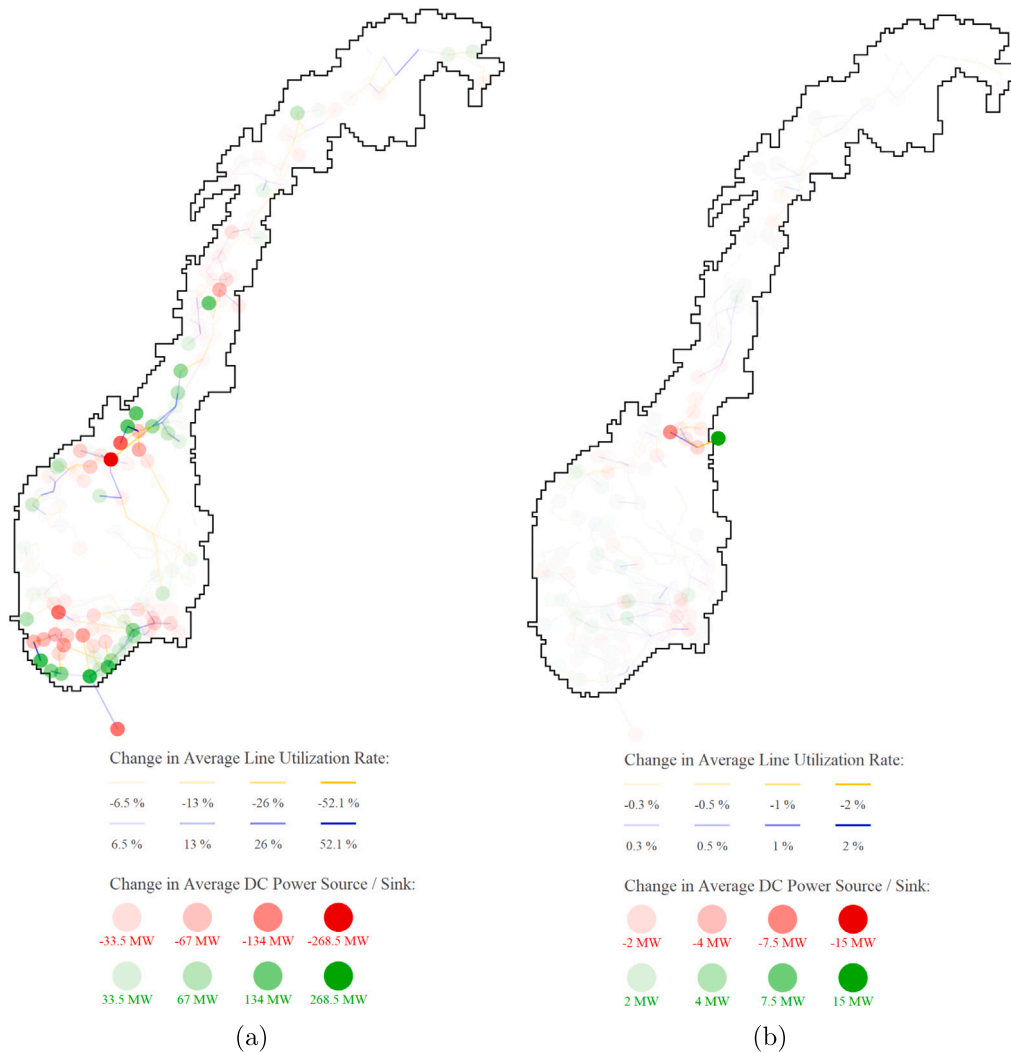
Fig. 4. Operation conditions of the transmission power network after redispatch in the Reference Scenario between (a) Winter weeks and (b) Summer weeks. The utilization rate of the transmission power lines is calculated based on the constraints of the DC power flow model of the TSO (as described in Section 3.5.2).

To conclude, for the TSO and DSOs, the participation of active end-users in the power system not only can increase the economic efficiency of redispatch, but they can also alleviate some of the extreme operational conditions on the power network. TSO and DSOs can take note on this benefit when determining the necessary conventional flexibility resources needed for their operations.

5. Conclusion

In this paper, we investigate the economic values of end-users participation in the power market with a TSO-DSO coordination scheme and how this participation affect the operation of the power system. To this end, we present a model for the power market in Norway that incorporates TSO-DSO coordination with a detailed emphasis on the distribution network and end-users. During the process, we model the distribution power networks and end-users with a high spatial resolution as well as model the entire Norwegian power system.

The findings demonstrate that the introduction of the TSO-DSO coordination scheme, coupled with active end-user participation, yields a modest reduction in the total operational cost of the system within the simulated time periods. However, the effects on cost in the EOM and redispatch counterbalance each other. As a result, active end-users, who contribute flexibility to the system, can benefit from lower electricity prices even without additional support schemes. Conversely, other types of end-users do not experience significant changes in electricity

prices when active end-users provide flexibility for redispatch. More-over, while the implementation of the TSO-DSO coordination scheme and active end-users does not substantially impact average operational conditions over the simulated time periods, it effectively mitigates spatial imbalances between supply and demand at critical time slices and reduces temporal variations in residual demand profiles within certain DSOs.

These outcomes highlight the potential incentives for active end-users and the benefits they can bring to the power system through their participation in the power market with TSO-DSO coordination scheme. Thus, the inclusion of active end-users may enhance social acceptance among policy makers and system operators when introducing this coordination scheme.

This paper investigated the operation of the power system with representative weeks in summer and winter. Future research should take a longer timescale. That is, end-users and power market players should consider their investment and operational strategies according to the behaviors of other agents and the general conditions in the power system. Additionally, future research on TSO-DSO coordination should encompass a thorough assessment of power system reliability, considering the increasing complexity of integrated grids and the need to ensure reliable and secure operations even in the face of contingencies.

Finally, the application of various power system models to the entire Norwegian power system is itself interesting and noteworthy. For readers who are conducting similar studies, here are some important

Fig. 5. Change of operation conditions of the transmission power network after redispatch in the Fully Flexible Scenario (compared with those in the Reference Scenario) (a) at 11:00 12 Jan and (b) between 01 Jan to 14 Jan (averaged value).
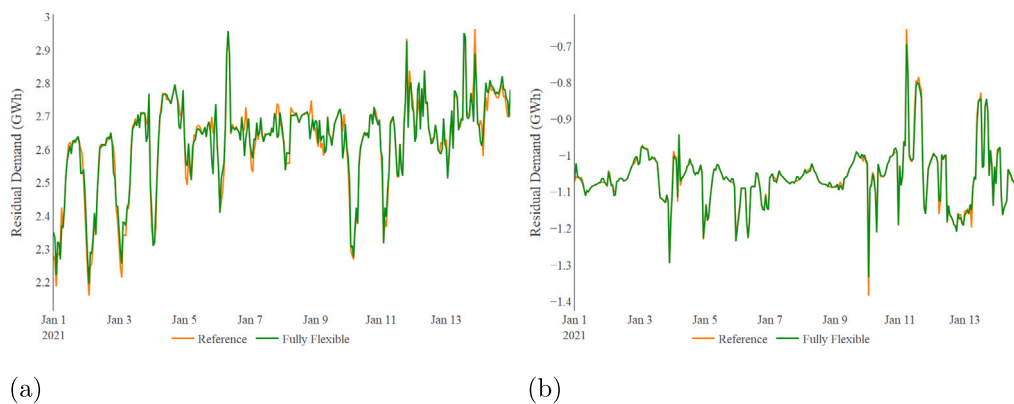

Fig. 6. Residual demand profiles in the Reference Scenario and the Fully Flexible Scenario in winter weeks (a) DSO #2 in the model (in Oslo) and (b) DSO #46 in the model (in Rogaland).

points in this paper that might be possible to generalize or compare with other power systems:

- DSOs seem to not play an active role in enabling or deterring end-use flexibility. In Norway (as of 2021), DSOs have some distributed flexibility that is mainly useful for TSO operations.

That is, the DSO filtering occurrence is low in our results. Flexibility needs for the distribution network could play a central role on other power systems or undermine TSO-DSO coordination in favor of local flexibility balance.

- The paper considers both EOM and redispatch operations. In an active end-user paradigm, these actors will have the capability to

participate and optimize their consumption on the EOM as well as (later on) contribute to TSO-DSO coordination. This insight is explored in the paper as it is overlooked in other paper and other power systems cases.

- The Norwegian power system is characterized by the high share of renewable power plants, and a less flexible conventional power plant fleet may lead to even higher values for active end-users for other power systems.
- The results in this paper suggest that the effect of active end-user participation on the power system can vary between different seasons. Active end-users contribute more to system costs reduction in the winter weeks. This might be generalizable to places with similar seasonal characteristics.

CRediT authorship contribution statement

Dung-Bai Yen: Conceptualization, Methodology, Data curation, Visualization, Writing – original draft. **Pedro Crespo del Granado:** Conceptualization, Writing – review & editing, Supervision. **Maria Lavrutich:** Writing – review & editing, Supervision, Project administration.

Declaration of competing interest

The authors declare the following financial interests/personal relationships which may be considered as potential competing interests: Dung-Bai Yen reports financial support was provided by Research Council of Norway.

Data availability

This research has been performed based on open-access data. Data management and results visualization are performed with R and Python, while the simulation is written in C++. The source codes can be found on GitHub: https://github.com/TonyYenTWN/trEnD.

Acknowledgments

Appendix A. Estimation of the electricity demand field per capita

In our model, the electricity demand per capita, μ, is treated as a spatiotemporal field in a real L^2 space. We estimate this spatiotemporal field by using the technique known as the Bayesian maximum entropy method [37,38] in the literature. The assumptions we use for the estimation of μ are

1. At each spatial point x and t, $\mu(x,t)$ obeys a certain type of probability distribution with non-negative support and finite variance.
2. There exists a bijective mapping $m : \mu(x,t) \mapsto v(x,t)$ at each spatial point x and t such that $v(x,t)$ obeys a standard normal distribution. In addition, at each time t the covariance function of $v(t)$ between 2 spatial points, $\text{Cov}(x_1, x_2)$, is a known function of the geodesic distance between x_1 and x_2. Time-dependency of the covariance function and autocovariance of $v(x)$ at a spatial point x is not considered in the model but can be included in the future.

3. At each time t, we have equality constraints $C_k(t) = \int c_k(x)\mu(x,t) \, dx$ from measurement, where c_k is the covector associated to equality constraint k. In our case, c_k is the population density field within bidding zone k in Norway while $C_k(t)$ is the aggregated demand of that bidding zone at time t.

Following [37], we can first infer the prior probability density function of $v(t)$, $p(v(t))$, by using the principle of maximum entropy. For a random variable field with known mean and covariance:

$$p(v(t)) \propto \exp\left(-\frac{1}{2} \iint v(x_1,t)v(x_2,t)\text{Cov}^{-1}(x_1,x_2)dx_1 dx_2\right) \quad \text{(A.1)}$$

Cov^{-1} in Eq. (A.1) should be understood by virtue of eigen-decomposition: suppose we have obtained the set of orthogonal eigenfunctions for Cov via the Kosambi–Karhunen–Loève theorem, such that

$$\int \text{Cov}(x_1,x_2)\phi_n(x_1)dx_1 = \kappa_n \phi_n(x_2) \quad \text{(A.2)}$$

where ϕ_n is the nth function in the set of eigenfunctions of $\text{Cov}(x_1, x_2)$; consequently, applying Cov^{-1} on ϕ_n will result in

$$\int \text{Cov}^{-1}(x_1,x_2)\phi_n(x_1)dx_1 = \kappa_n^{-1} \phi_n(x_2) \quad \text{(A.3)}$$

Then, at time t, we can infer the posterior probability density function of the entire random field v, $p'(v(t))$,:

$$p'(v(t)) = \frac{p(v(t))}{\int_\Omega p(v(t))dv(t)} \quad \text{(A.4)}$$

Here Ω is the set of $v(t)$ such that the equality constraints $C_k(t) = \int c_k(x)\mu(x,t)dx$ hold.

Finally, we can estimate $\mu(t)$ from the posterior of $v(t)$ and the inverse mapping of m, $m^{-1} : v \mapsto \mu$. Of all the statistic parameters of $p'(v(t))$, the mode is perhaps the most simple one to compute. This will be equivalent to finding $v(t)$ that solves the following problem:

$$\min_{v(t),\lambda(t)} \quad \frac{1}{2} \iint v(x_1,t)v(x_2,t)\text{Cov}^{-1}(x_1,x_2)dx_1 dx_2$$
$$+ \sum_k \lambda_k(t) \int c_k(t) \, m^{-1}(v(x,t))dx \quad \text{(A.5)}$$

Here $\lambda_k(t)$ is the Lagrangian multiplier for equality constraint k at time t, which are found by solving the equality constraints:

$$\int c_k(t) \, m^{-1}(v(x,t))dx = C_k(t) \quad \text{(A.6)}$$

Once we obtain $\mu(x,t)$ with Eq. (A.5) and Eq. (A.6), we assume that this is the default electricity demand per capita for all the end-users at the spatial point x at time t.

For simplicity, in our model we choose $\mu(x,t)$ to follow a Weibull distribution with a probability density function of the form:

$$f(\mu(x,t); \mu_0(x)) \propto \mu(x,t) \exp\left(-\left(\frac{\mu(x,t)}{\mu_0(x)}\right)^2\right) \quad \text{(A.7)}$$

Here $\mu_0(x)$ is a predetermined parameter field inferred from annual mean values of the original electricity demand data. The mapping between $\mu(x,t)$ and $v(x,t)$ is done by pairing the values of μ^* and v^* such that $F_{\mu(x,t)}(\mu^*) = F_{v(x,t)}(v^*)$, where $F_{\mu(x,t)}$ and $F_{v(x,t)}$ are the cumulative distribution functions for $\mu(x,t)$ and $v(x,t)$, respectively.

Appendix B. Stylized modeling of the distribution power networks

We model the distribution power network under the following assumptions:

1. The distribution power network lies in a 2 dimensional Euclidean space $\mathbf{R}^2$.
2. At any spatial point x in $\mathbf{R}^2$, the number density per unit area of power lines in the distribution power network with 1 end located at x is ρ_N.

Table 8
Summary of the key findings of the TSO-DSO coordination literature cited.

Literature	Key findings
[9]	TSO-DSO coordination for redispatch can save up to 300 million Euros in Germany in 2030.
[11]	The use of flexibility resources enables more options for DSOs to solve network issues, but liquidity might be a concern for local markets.
[13]	A hierarchy model can enable both TSO and DSO to utilize local resources, but the priority of DSO to use local resources might lead to sub-optimal solutions.
[14]	A bi-level coordination mechanism can benefit transmission expansion by allowing TSO to postpone upgrades, so long as the power exchange limits between the two levels are sufficient.
[15]	With flexibility activated through spatio-temporally varying prices in local energy markets, certain barriers regarding standardization can be overcome, but many barriers within end-users' lifestyle and administrative categories still exist for adoption of local flexibility markets.
[16]	An interface optimizer acting as a leader in a Stackelberg game for the DSO and DSO-level flexible resources to follow and adopt optimal day-ahead schedule accordingly can lead to social welfare close to optimal.
[17]	In a novel TSO–DSO coordination mechanism enabling the procurement of ancillary services by TSO from its DSOs in day-ahead operation, DSOs can provide substantial active and reactive power flexibility. TSO procures mostly downward flexibility from active distribution systems.
[20]	Demand-side flexibility provided by individual buildings were integrated into the traditional process of reserve scheduling. Some traditional reserve scheduling services could be replaced under this Building-to-grid (BtG) integration framework, without jeopardizing the stability of the grid or violating thermal comfort constraints of buildings.
[21]	Flexibility from customers in field was demonstrated to successfully alleviate network congestion, reduce system costs while keeping a secure operation. Engagement among stakeholders, customer-friendly technical requirements, and timing of the market were among the key factors listed in the study for the success of these flexibility markets.
[22]	DR programs, distributed storage and other DERs together provided reduced total costs of the system by 1%. Half of the decrease resulted from reduced number of start-ups and shutdowns of conventional power plants.

3. At any spatial point x in $\mathbf{R}^2$, the power lines with 1 end located at x are isotropic.

4. At any spatial point x in $\mathbf{R}^2$, the probability density function of the length of the power lines with 1 end located at x obeys a Pareto distribution with cumulative distribution function: $F(l) = 1 - \left(\frac{l}{l_m}\right)^{1-\alpha}$, where l is the length of the power lines, l_m the cutoff length of the power lines to be considered for the desired spatial resolution, and $\alpha > 1$. Differentiate $F(l)$ yields the probability density function for l: $f(l) = (\alpha - 1)l_m^{\alpha-1}l^{-\alpha}$.

5. The impedance per unit length of power lines in the distribution power network is z.

Under the above assumptions, we can derive the power flow equation of the distribution power network:

$$\Delta I(x_1) = \frac{\rho_N(\alpha-1)l_m^{\alpha-1}}{2\pi z} \int_{\mathbf{R}^2 \setminus \mathbf{B}_{l_m}(x_1)} \frac{V(x_1) - V(x_2)}{|x_1 - x_2|^{2+\alpha}} dx_2 \qquad (B.1)$$

Here $\Delta I(x_1)$ is the current source at x_1 (if $\Delta I(x_1) < 0$, then there is a current sink at x_1), $V(x_1)$ and $V(x_2)$ the voltage values at x_1 and x_2 respectively, and $\mathbf{B}_{l_m}(x_1)$ is a ball with radius l_m centered at x_1. Note that in the limit where $l_m \to 0$, the right hand side of Eq. (B.1) can be interpreted as a fractional Laplacian operator acting on the voltage field in $\mathbf{R}^2$, up to some constant [39], assuming $\rho_N l_m^{\alpha-1}$ is held fixed (which leads to the reasonable implication that ρ_N increases as we decrease l_m to achieve a higher spatial resolution).

Eq. (B.1) can be discretized with the desired spatial resolution to obtain the nodal admittance matrices of the distribution power networks in the model. We assume there are no power line connections between distribution power networks, so the nodal admittance matrix of each distribution power network can be modeled separately.

Appendix C. Summary of key findings in cited literature

See Table 8.

Table 9
Summary of symbols used in the paper. Sorted by order of first appearance.

Symbol	Description
$\mathcal{T}_i$	The foresight time interval of the end-user i.
$M^s(x,t)$, $M^d(x,t)$	The end-users' expected procurement (retailer) price for electricity production (demand) at spatial point x and time t.
$U_i^s(t)$, $U_i^d(t)$	The scheduled production (demand) quantity of end-user i.
$\{E\}(x)$	The set of end-users at spatial point x.
$D_{0,i}(t)$	The inflexible electricity demand of end-user i at time t.
$U_i^b(t)$, $U_i^{ev}(t)$, $U_i^{sa}(t)$	The electricity produced (consumed) from the BESS, home-charging EV, and smart appliance owned by end-user i at time t.
$\eta_i^{ch,b}$, $\eta_i^{dc,b}$	The charge (discharge) efficiency for the BESS owned by end-user i.
$ch_i^b(t)$, $dc_i^b(t)$	The charge (discharge) volume of the BESS owned by end-user i at time t.
$soc_i^b(t)$	The state of charge (SOC) of the BESS owned by end-user i at time t.
$\eta_i^{ch,ev}$, $\eta_i^{dc,ev}$	The charge (discharge) efficiency for the EV owned by end-user i.
$ch_i^{ev}(t)$, $dc_i^{ev}(t)$	The charge (discharge) volume of the EV owned by end-user i at time t.
$soc_i^{ev}(t)$	The SOC of the EV owned by end-user i at time t.
$d_i^{ev}(t)$	The electricity consumed for providing transportation service of the EV owned by end-user i at time t.
$d_i^{sa}(t_1, t_2)$	The flexible demand shifted from t_1 to t_2 via smart appliances by end-user i.
Δt	The maximum possible time shift.
$d_i^{sa}(t)$	The unfulfilled default demand profile at time t of the smart appliances for end-user i.
$\{A\}_{\mathbb{D}}$	The set of all the market participants in the operational area of a particular DSO $\mathbb{D}$.
$\{\mathbb{B}\}_i$	The set of bids submitted by a particular market participant i.
B^{max}	The maximum bidding price in the EOM.
$\hat{B}_j^s(t)$	The equivalent bidding price of supply bid j considered in the DSO problem at time t.
$\hat{Q}_j^s(t)$	The quantity of supply bid j allowed to enter the redispatch problem of the TSO at time t.

(continued on next page)

Table 9 (*continued*).

Symbol	Description
$[\mathcal{Y}]_{\mathbb{D}}$	The line admittance matrix of the distribution power network in the operation area of a particular DSO $\mathbb{D}$.
$[\mathcal{I}]_{\mathbb{D}}$	The signed incidence matrix of the network in the operation area of a particular DSO $\mathbb{D}$.
$\{\theta\}_{\mathbb{D}}(t)$	The phase angles at the nodes of the network in the operation area of a particular DSO $\mathbb{D}$ at time t.
$\{I\}_{\mathbb{D}}(t)$	The DC power flow on the power lines of the network in the operation area of a particular DSO $\mathbb{D}$ at time t.
$[Y]_{\mathbb{D}}$	The nodal admittance matrix of the network in the operation area of a particular DSO $\mathbb{D}$.
$\{S\}_{\mathbb{D}}(t)$	The power source (sink) at the nodes of the network in the operation area of a particular DSO $\mathbb{D}$ at time t.
$[\mathcal{Y}_{sh}]_{\mathbb{D}}$	The shunt admittance matrix of the nodes in $\mathbb{D}$.
$\{\mathbf{N}\}_{\mathbb{D}}$	The set of nodes in the DSO $\mathbb{D}$.
$\{A\}_n$	The market participants at node n.
$S_n(t)$	The power source at the node n at time t.
$\tilde{B}_j^d(t)$	The equivalent bidding price of demand bid j considered in the DSO problem at time t.
$\tilde{Q}_j^d(t)$	The quantity of demand bid j allowed to enter the redispatch problem of the TSO at time t.
$\{Z\}$	The set of bidding zones involved in the EOM.
$\{A\}_z$	The set of all the market participants in bidding zone z.
$B_j^d(t),\ B_j^s(t)$	The participant-determined bidding price of demand (supply) of bid j at time t.
$Q_j^d(t),\ Q_j^s(t)$	The cleared bidding quantity of demand (supply) of bid j at time t in the EOM.
$F_{z\zeta}$	The cross-border flow from bidding zone z to bidding zone ζ at time t.
$\tilde{Q}_j^d(t),\ \tilde{Q}_j^s(t)$	The confirmed bidding quantity of demand (supply) of bid j at time t.
$[\mathcal{Y}]_{\mathbb{T}}$	The line admittance matrix of the transmission power network $\mathbb{T}$.
$[\mathcal{I}]_{\mathbb{T}}$	The signed incidence matrix of the network in the transmission power network $\mathbb{T}$.
$\{\theta\}_{\mathbb{T}}(t)$	The phase angles at the nodes of the transmission power network $\mathbb{T}$ at time t.
$\{I\}_{\mathbb{T}}(t)$	The DC power flow on the power lines of the transmission power network $\mathbb{T}$ at time t.
$[Y]_{\mathbb{T}}$	The nodal admittance matrix of the transmission power network $\mathbb{T}$.
$\{S\}_{\mathbb{T}}(t)$	The power source (sink) at the nodes of the transmission power network $\mathbb{T}$ at time t.
$[\mathcal{Y}_{sh}]_{\mathbb{T}}$	The shunt admittance matrix of the nodes in $\mathbb{T}$.
$\{\mathbf{N}\}_{\mathbb{T}}$	The set of nodes in $\mathbb{T}$.
$\mu(x,t)$	The electricity demand per capita at spatial point x at time t.
$\nu(x,t)$	A bijective mapping from $\mu(x,t)$. Note that the alternative notation $\nu(t)$ refers to the spatial field at fixed time t, while $\nu(x)$ refers to the time series at fixed spatial point x.
$\mathrm{Cov}(x_1,x_2)$	The covariance function of $\nu(t)$ between 2 spatial points at a fixed time.
$C_k(t)$	Equality constraints the spatio-temporal field μ must obey.
c_k	The covector associated to equality constraint k
$p(\nu(t))$	The prior probability density function of $\nu(t)$.
ϕ_n	The nth function in the set of eigenfunctions of $\mathrm{Cov}(x_1,x_2)$.
$p'(\nu(t))$	The posterior probability density function of $\nu(t)$.
Ω	The set of $\nu(t)$ such that the equality constraints $C_k(t) = \int c_k(x)\mu(x,t)dx$ hold.
$\lambda_k(t)$	The Lagrangian multiplier for equality constraint k at time t.
$\mu_0(x)$	A predetermined parameter field inferred from annual mean values of the original electricity demand data.
$\mathrm{F}_{\mu(x,t)},\ \mathrm{F}_{\nu(x,t)}$	The cumulative distribution functions for $\mu(x,t)$ and $\nu(x,t)$
ρ_N	The number density per unit area of power lines in the distribution power network with 1 end located at x
l_{m}	The cutoff length of the power lines to be considered for the desired spatial resolution.
z	The impedance per unit length of power lines in the distribution power network.
$\Delta I(x_1)$	The current source at x_1.
$V(x_1)$	The voltage values at x_1.
$\mathbf{B}_{l_{\mathrm{m}}}(x_1)$	A ball with radius l_{m} centered at x_1.

Appendix D. Summary of symbols used in the paper

See Table 9.

References

[1] L. Lind, R. Cossent, J.P. Chaves-Ávila, T. Gómez San Román, Transmission and distribution coordination in power systems with high shares of distributed energy resources providing balancing and congestion management services, Wiley Interdiscip. Rev.: Energy Environ. 8 (6) (2019) e357.

[2] T. Alazemi, M. Darwish, M. Radi, Tso/dso coordination for res integration: A systematic literature review, Energies 15 (19) (2022) 7312.

[3] J. Stekli, L. Bai, U. Cali, U. Halden, M.F. Dynge, Distributed energy resource participation in electricity markets: A review of approaches, modeling, and enabling information and communication technologies, Energy Strategy Rev. 43 (2022) 100940.

[4] C. Silva, P. Faria, Z. Vale, J. Corchado, Demand response performance and uncertainty: A systematic literature review, Energy Strategy Rev. 41 (2022) 100857.

[5] C. Eid, P. Codani, Y. Perez, J. Reneses, R. Hakvoort, Managing electric flexibility from distributed energy resources: A review of incentives for market design, Renew. Sustain. Energy Rev. 64 (2016) 237–247.

[6] J. Villar, R. Bessa, M. Matos, Flexibility products and markets: Literature review, Electr. Power Syst. Res. 154 (2018) 329–340.

[7] D. Mariano-Hernández, L. Hernández-Callejo, A. Zorita-Lamadrid, O. Duque-Pérez, F.S. García, A review of strategies for building energy management system: Model predictive control, demand side management, optimization, and fault detect & diagnosis, J. Build. Eng. 33 (2021) 101692.

[8] S. Panda, S. Mohanty, P.K. Rout, B.K. Sahu, M. Bajaj, H.M. Zawbaa, S. Kamel, Residential demand side management model, optimization and future perspective: A review, Energy Rep. 8 (2022) 3727–3766.

[9] S. Pearson, S. Wellnitz, P.C. del Granado, N. Hashemipour, The value of tso-dso coordination in re-dispatch with flexible decentralized energy sources: Insights for germany in 2030, Appl. Energy 326 (2022) 119905.

[10] A.G. Givisiez, K. Petrou, L.F. Ochoa, A review on tso-dso coordination models and solution techniques, Electr. Power Syst. Res. 189 (2020) 106659.

[11] M. Rossi, G. Migliavacca, G. Viganò, D. Siface, C. Madina, I. Gomez, I. Kockar, A. Morch, Tso-dso coordination to acquire services from distribution grids: Simulations, cost–benefit analysis and regulatory conclusions from the smartnet project, Electr. Power Syst. Res. 189 (2020) 106700.

[12] L. Mendicino, D. Menniti, A. Pinnarelli, N. Sorrentino, P. Vizza, C. Alberti, F. Dura, Dso flexibility market framework for renewable energy community of nanogrids, Energies 14 (12) (2021).

[13] M. Khojasteh, P. Faria, F. Lezama, Z. Vale, A hierarchy model to use local resources by dso and tso in the balancing market, Energy 267 (2023) 126461.

[14] J. Liu, P.P. Zeng, H. Xing, Y. Li, Q. Wu, Hierarchical duality-based planning of transmission networks coordinating active distribution network operation, Energy 213 (2020) 118488.

[15] G. Pressmair, E. Kapassa, D. Casado-Mansilla, C.E. Borges, M. Themistocleous, Overcoming barriers for the adoption of local energy and flexibility markets: A user-centric and hybrid model, J. Clean. Prod. 317 (2021) 128323.

[16] A. Hermann, T.V. Jensen, J.Ø. stergaard, J. Kazempour, A complementarity model for electric power transmission-distribution coordination under uncertainty, European J. Oper. Res. (2021).

[17] M. Usman, M.I. Alizadeh, F. Capitanescu, I.-I. Avramidis, A.G. Madureira, A novel two-stage tso–dso coordination approach for managing congestion and voltages, Int. J. Electr. Power Energy Syst. 147 (2023) 108887.

[18] CINELDI, Cineldi research: interaction dso/tso, 2022, https://www.sintef.no/projectweb/cineldi/research/interaction_dso-tso/. Last Accessed 20 December 2022.

[19] G.H. Kjølle, K. Sand, E. Gramme, Scenarios for the future electricity distribution grid, CIRED - Open Access Proce. J. (2021).

[20] V. Rostampour, T.S. Badings, J.M.A. Scherpen, Demand flexibility management for buildings-to-grid integration with uncertain generation, Energies 13 (24) (2020).

[21] Y. Ruwaida, J.P. Chaves-Avila, N. Etherden, I. Gomez-Arriola, G. Gürses-Tran, K. Kessels, C. Madina, A. Sanjab, M. Santos-Mugica, D.N. Trakas, et al., Tso-dso-customer coordination for purchasing flexibility system services: Challenges and lessons learned from a demonstration in Sweden, IEEE Trans. Power Syst. 38 (2) (2022) 1881–1893.

[22] H.H. Grøttum, S.F. Bjerland, P.C. del Granado, R. Egging, Modelling tso-dso coordination: the value of distributed flexible resources to the power system, in: 2019 16th International Conference on the European Energy Market, (EEM), 2019, pp. 1–6.

[23] H. Khajeh, H. Laaksonen, A.S. Gazafroudi, M. Shafie-khah, Towards flexibility trading at tso-dso-customer levels: A review, Energies 13 (1) (2020).

[24] T. Freire-Barceló, F. Martín-Martínez, Á. Sánchez-Miralles, A literature review of explicit demand flexibility providing energy services, Electr. Power Syst. Res. 209 (2022) 107953.

[25] P. Crespo del Granado, R.H. van Nieuwkoop, E.G. Kardakos, C. Schaffner, Modelling the energy transition: A nexus of energy system and economic models, Energy Strategy Rev. 20 (2018) 229–235.

[26] M. Troncia, J.P. Chaves Ávila, C. Damas Silva, H. Gerard, G. Willeghems, Market-based tso–dso coordination: A comprehensive theoretical market framework and lessons from real-world implementations, Energies 16 (19) (2023) 6939.

[27] Solar Learning Center, How long can solar battery power a house during an outage?, 2023, https://www.solar.com/learn/how-long-can-a-battery-provide-power-during-an-outage/. Last Accessed 7 March 2023.

[28] Joju Solar, Batteries faqs, 2023, https://www.jojusolar.co.uk/faqs-batteries/. Last Accessed 7 March 2023.

[29] E.F. Norway, Energy use by sector, 2023, https://energifaktanorge.no/en/norsk-energibruk/energibruken-i-ulike-sektorer/. Last Accessed 22 May 2023.

[30] M.U. Hashmi, A. Mukhopadhyay, A. Bušić, J. Elias, Optimal control of storage under time varying electricity prices, in: 2017 IEEE International Conference on Smart Grid Communications, (SmartGridComm), IEEE, 2017, pp. 134–140.

[31] C. Corinaldesi, D. Schwabeneder, G. Lettner, H. Auer, A rolling horizon approach for real-time trading and portfolio optimization of end-user flexibilities, Sustain. Energy, Grids Netw. 24 (2020) 100392.

[32] E.F. Norway, The electricity grid, 2023, https://energifaktanorge.no/en/norsk-energiforsyning/kraftnett/. Last Accessed 12 November 2023.

[33] A. Trias, Fundamentals of the holomorphic embedding load-flow method, 2015.

[34] ENTSO-E, Entso-e transparency platform, 2022, https://transparency.entsoe.eu/. Last Accessed 11 October 2022.

[35] Elexon, Elexon portal, 2022, https://www.elexonportal.co.uk/. Last Accessed 11 October 2022.

[36] NVE, Nedlasting av fagdata fra nve, 2022, https://nedlasting.nve.no/gis/. Last Accessed 14 December 2022.

[37] J. He, A. Kolovos, Bayesian maximum entropy approach and its applications: A review, Stoch. Environ. Res. Risk Assess. 32 (4) (2018) 859–877.

[38] G. Christakos, A bayesian/maximum-entropy view to the spatial estimation problem, Math. Geol. 22 (7) (1990) 763–777.

[39] A. Lischke, G. Pang, M. Gulian, F. Song, C. Glusa, X. Zheng, Z. Mao, W. Cai, M.M. Meerschaert, M. Ainsworth, G.E. Karniadakis, What is the fractional Laplacian? A comparative review with new results, J. Comput. Phys. 404 (2020) 109009.